Pulsar scintillations from corrugated reconnection sheets in the ISM

Ue-Li Pen,[1]* Yuri Levin,[2]†

18 July 2012

ABSTRACT

We show that surface waves along interstellar current sheets closely aligned with the line of sight lead to pulsar scintillation properties consistent with those observed. By contrast with previously considered scintillation drivers, our mechanism naturally produces the length and density scales of the ISM scattering lenses that are required to explain the magnitude and dynamical spectrum of the scintillations. In our picture, the parts of warm ionized interstellar medium that are responsible for the scintillations are relatively quiescent, with scintillation and scattering resulting from weak waves propagating along magnetic domain boundary current sheets, which are both expected from helicity conservation and have been observed in numerical simulations. The model quantitatively predicts the spacing and amplitudes of inverted parabolic arcs seen in Fourier-transformed dynamical spectra of strongly scintillating pulsars Multi-Frequency, multi-epoch VLBI observations can quantitatively test this picture. If successful, in addition to mapping the ISM, this opens the door to precise nanoarc-second pulsar astrometry, distance measurements, and emission studies using these 100AU interferometers in the sky. THE LATEST STATEMENT IS CURRENTLY NOT BACKED UP BY ANYTHING IN THE PAPER.

Key words: Interstellar Medium, reconnection, extreme scattering events ARE WE EVEN MENTIONING THE EXTREME SCATTERING EVENTS?

1 INTRODUCTION: **OBSERVATIONS AND THEORETICAL CHALLENGES**

Pulsars provide a precision probe of the ionized interstellar medium (IISM). The propagation speed of radio waves depends on the density of free electrons, which results in refractive and diffractive abberation and scattering.

The structure of the IISM interstellar medium has remained enigmatic. Five decades of pulsar scintillation observations Scheuer (1968) have resulted in problematic physical requirements I THINK WE NEED TO GIVE SEVERAL MORE CITATIONS FOR THE FIVE DECADES. Current observations have demonstrated that much of the scattering is dominated by a small number of very localized lensing screens (Brisken et al. 2010) along the line of sight WHAT IS THE STRONGEST EVIDENCE FOR THIS? I THOUGHT THIS WAS PARABOLIC ARCS. IF SO WE SHOULD SAY SMTHG LIKE

Major observational progress of the ISM scintillations has been achieved through the Stinebring et al.Stinebring et al. (2001) detection of parabolic structures in the Fourier-

tranformed dynamical spectra of strongly scintillating pulsars. These parabolic structures imply that for these pulsars the radio-wave scattering occures mostly within one or several thin screens (Walker et al. (2004); Cordes et al. (2006); Walker et al. (2008)). Moreover, the multiple "inverted parabolae" (Hill et al. (2005)) **what is Hill&Stinebring 2007?** (Hill & Stinebring 2005, 2007) show that the scattering inside the screen is strongly inhomogeneous but instead occures in localized clumps. The latter was recently confirmed by Brisken et al.Brisken et al. (2010) who have obtained the VLBI scattering image PSR B0834+06. They have found that not only the scattering image was clumpy but that the clumps lined up along a thin line. (SHOULD WE ALSO MENTION THE SECOND CLUMP?) All of these observational facts present a major challenge for theoretical interpretation where the scattering is caused by a turbulent cascade. In particular, (1) the origin of the screens is unexplained, and (2) the strongly non-gaussian scattering on the requires AU-size regions of which are over-pressurized by factors of $\sim 10^3$ relative to the ambient warm ISM (REFERENCE?); no conventional physical mechanism has been proposed for how such regions may be formed.

Radio-wave scattering by non-turbulent large-scale refractive structures has been previously considered by Ro-

* E-mail: pen@cita.utoronto.ca
† E-mail: yuri.levin@monash.edu

mani, Blandford, & Cordes (1987), mostly in the context of the so-called extreme-scattering events observed by Fiedler et al. Recently, Goldreich and Sridhar (2006) proposed that the image of the SgrA* radio-source is strongly scattered by several reconnection sheets that are closely aligned with the line of sight to SgrA*. In this paper, we develop further the Goldreich & Sridhar's (2006) idea [see also Pen & King 2011] and apply it to construct a quantitative picture of pulsar scintillations. Namely, we consider a scenario where the pulsar radio-wave scattering occurs due to several *weakly corrugated* reconnection sheets that are closely aligned with the line of sight to the pulsar. We show that this scenario provides compelling explanations for previously unexplained features of the scintillations: (1) the "scattering screens" are simply effective descriptions of such sheets; their location is marked approximately by the sheets' intersections with the line of sight, (2) "the scattering clumps" correspond to those parts of sheet folds where the sheet is parallel to the line of sight; the strength of the scattering follows a strongly non-Gaussian distribution, even though the corrugation itself is assumed to be a realization of a Gaussian distribution, and (3) the strong non-isotropy of the Brisken et al. 2010 image is a consequence of the sheet's inclination, with the clump locations aligned along the sheet's line of nodes. The plan of the paper is as follows: in the next section we briefly describe the origin of the reconnection sheets, in section 3 we derive the model for the fold statistics, in section 4 we derive the lensing by the corrugated sheet, and in section 5 we compute the Fourier-transformed dynamical spectrum and demonstrate the parabolic structures. In section 6 we conclude.

UE-LI, I WOULD PROPOSE TO MAKE THE NEXT 3 SECTIONS INTO 3 SUBSECTIONS OF A LARGER SECTION CALLED "ASTROPHYSICAL PICTURE". I'D ALSO PUT THE "TWO REGIMES OF LENSING" SUBSECTION LAST SINCE NOW IT SORT OF COMES OUT OF NOWHERE.

2   ASTROPHYSICAL PICTURE

2.1   Two Regimes of Lensing: Diffractive vs Refractive

Two regimes to generate pulsar scintillation have been considered. In the diffractive !!picture!! **regime**, the scattering/lensing angle is determined by the size of structure in the medium, compared to the wavelength λ: $\theta = 2\pi\lambda k$. WE HAVE TO DEFINE k. IT IS THE CHARECTERISTIC WAVEVECTOR OF A SCATTERING STRUCTURE PERPENDICULAR TO THE LINE OF SIGHT, RIGHT? The amplitude of !!each!! scattered !!structure!! **image** IN THE PREVIOUS SENTENCE WE USED "STRUCTURE" AS IN PERTURBATION IN THE ISM, BUT HERE WE USE STRUCTURE AS IN PERTURBATION IN THE SCATTERING IMAGE. FORM THE POINT OF VIEW OF THE LANGUAGE, THESE ARE DISTINCT is determined by the !!depth!! **amplitude** of the **wavefront** modulation **caused by the scattering structure**. To explain the observed angles in the range $1 - 100$ mas at wavelength ~ 1m, requires structures in the ISM on scales of order 10^{6-8}m. This imposes unexpected properties on the

IISM?, since it is much smaller than the coloumb mean free path of free electrons. In this scenario, the angular image of a pulsar, and therefore its dynamic spectrum, are superpositions of many CAN WE ESTIMATE HOW MANY? IS THIS NOT JUST $(AU/10^8 M)$ 10^3 FOR A 1-D SCATTERING IMAGE? weak structures, and are expected to be roughly gaussian. The parabolically structured 2-D power spectrum of the dynamic spectrum, and the VLBI image of the scattering disk, are inconsistent with such a picture, at least for the long-lag (ms) structures.

A second mechanism is due to refractive lensing. In this scenario, the bending angle is determined by Snell's law, i.e. the change in refractive index and the angles of incidence. The refractive index of a plasma is $n = 1/\sqrt{1 - \omega_p^2/\omega^2}$, with plasma frequency $\omega_p = \sqrt{n_e e^2/\epsilon_0 m_e}$. Pulsar observations are done at frequency much higher than the plasma frequency, for which we expand $n - 1 \sim \frac{\omega_p^2}{2\omega^2} = 1.8 \times 10^{-8} n_e$. The observed scattered images at 20 mas require deflection angles of at least 40 mas, corresponding to $n_e \sim 10$ neglecting geometric alignment factors. The mean density of the IISM is typically 10^{-2} from dispersion measure.

This picture is also challenging to implement, since the observed scattering angles would naïvely require changes in free electron density of $\sim 10^3$ which are difficult to understand or confine.

Historically, refractive lensing was used to interpret long time variability, and diffraction for the minute time scale effects. Recently, it was understood that the refractive images result in an interference fringe patternWalker et al. (2004) which have similar time and frequency scales for flux modulation as diffractive effects. The frequency and time scaling was historically interpreted as related to an underlying stochastic diffractive process driven by turbulence. Goldreich & Sridhar (2006) showed that refractive lensing by aligned sheets results in scintillation similar to the diffractive picture.

!!The discovery of parabolic arcs(Stinebring et al. 2001) and inverted arclets has required the existence of localized refractive lenses. Direct VLBI imaging of the scattering screen(Brisken et al. 2010) demonstrate the presence of discrete isolated lenses, i.e. scattering points, which are all in a single thin sheet. This leads to physical challenges of confining these lenses. Various solutions have been proposed(Walker 2007; Pen & King 2012; Goldreich & Sridhar 2006).

In this paper, we expand the picture of current sheets, and consider perturbations.!!

2.2   Astrophysical Picture

The interstellar medium is stirred on scales of parsecs by various energetic processes, including supernovae, ionization fronts, spiral density waves, and other phenomena. These processes are generally short lived, and we conjecture after the stirring, the warm medium relaxes to an near-equilibrium configuration on small (several AU) scale. Current numerical simulations of the supernova-driven turbulence in the warm ISM of the Galaxy (e.g., Hill et al. 2011) do not have the resolution to tell how realistic this assumption is. In the presence of helicity, the equilibrium magnetic fields are configured as interlaced twisted tori, which are

long lived (Braithwaite & Spruit 2004). It has been shown by Gruzinov (2009) that a "generic magnetic equilibrium of an ideally conducting fluid contains a volume-filling set of singular current layers." In this picture, the magnetic fields are locally almost parallel, with discontinuous interface regions, a bit like magnetic domains in a ferromagnet. Singular current sheets have also been seen in the simulations of Schekochihin et al. (2004; ApJ, 612, 276 - YL.)

At the boundary between between magnetic field configurations, current sheets maintain the discontinuities. These current sheets have been proposed to dominate the scattering of radio sources (Goldreich & Sridhar 2006).

2.3 Surface Dynamics

The current sheet is physically thin, $<\sim$ AU. Theoretically, the thickness of current sheets is not understood, so we choose this scale to be thin enough to explain the smallest scale observed structures. On each side the magnetic field points in a different direction. The change in alvenic properties gives rise to surface wave (Jain & Roberts 1991; Joarder et al. 2009), whose amplitude decays exponentially with the distance to the current sheet and which are mathematically analogous to deep water ocean waves. The restoring force is due to the difference in magnetic field component projected along the wave vector. Like ocean waves, these waves penetrate about a wavelength into each side. We will be considering wavelengths of thousands of AU WHY?, so the **thickness of the** current sheet itself is neglible as far as the dynamics of the waves are concerned. Seen in projection along the aligned sheet, the projected wavelengths will be $\sim$ AU IS THIS BECAUSE THE ALIGNMENT ANGLE IS ~ 0.001? THIS IS THE FIRST TIME THAT THE MAGNITUDE OF THE ALIGNMENT ANGLE IS DISCUSSED; MAY NEED A BIT MORE EXPLANATION. The displacements are transverse to the wave vector, and perpendicular to the sheet. While alvenic in nature, the surface modes possess only one polarization, unlike bulk waves. These waves resemble a flag blowing in the wind. Disturbances travelling along the sheet are decoupled from bulk waves. Being confined to a sheet, the amplitude away from a source drops as $\propto 1/r$ instead of the normal inverse square law. A amplitude of order $\alpha\lambda$, HERE λ IS THE WAVENENGTH OF THE SURFACE WAVE BUT IT WAS PREVIOUSLY USED FOR THAT OF RADIO WAVES or about 10^{-3} of the wavelength is sufficient to cause the sheet to appear folded in projection.

2.4 Sheet statistics

Here we consider the lensing effect of a large ensemble of sheets. To understand the qualitative statistical behaviour, we consider infinitely thin round sheets, with one dimensional density corrugations on each sheet. This problem is effectively one dimensional.

3 FOLD STATISTICS

Alven waves dissipate on scales shorter than the proton mean free path WHICH IS WHAT IN THE WISM? REFERENCE?. We thus model the waves as a displacement
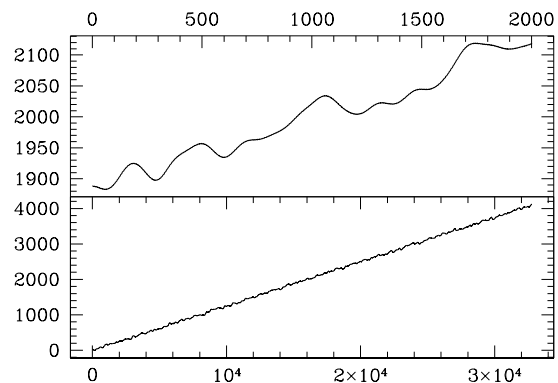
Figure 1. Sheet with transverse perturbations. The upper panel shows an zoomed version of a short section.

function $\zeta(x)$ which is a Gaussian random field with a correlation function that is a Gaussian, $\xi(r) = \langle\zeta(x)\zeta(x+r)\rangle = A^2\exp(-r^2/2\sigma^2)$, where **A is the mean amplitude of the displacement and** σ is the **surface-wave** dissipation scale. Figure 1 shows a realization of a sheet with a random fluctuations.

The current sheet has a reduced magnetic pressure and thus has a refractive index different from the ambient ISM. For simplicity, we assume here that the sheet has constant thickness, and consider its optical depth as is relevant for refractive lensing. In projection **along the line of sight**, the !!surface!! **column** density of the !!current!! sheet results in a highly non-Gaussian distribution. Figure 2 shows the **column** density distribution in a simulation. Folds occur when the gradient of the displacement is equal to minus 1 NO, IT IS $-\alpha$ WHERE ALPHA IS THE INCLINATION ANGLE. The correlation function of the gradients is the second derivative of the displacements. The number of crossings of -1 depends on the variance of the gradient field. The density of the folded sheet is proportionate to the length of gradient spent in the vicinity of -1, which is turn is proportionate to the reciprocal of the derivative of the gradient. This second derivative is also a Gaussian random field. The second derivative is uncorrelated with the first derivative. The one point PDF of the reciprocal of a Gaussian variable is

$$P(\rho) = \frac{\exp(-\frac{1}{2\rho^2})}{\sqrt{2\pi}\rho^2}. \tag{1}$$

UE-LI, I GET A DIFFERENT ANSWER. I DON'T HAVE THE FULL EXPRESSION, BUT ASYMPTOTICALLY THE HIGH-END TAIL IS CLEAR. LET θ BE THE ANGLE BETWEEN THE SCREEN AND THE LINE OF SIGHT. THEN THE OPTICAL DEPTH IS $\rho \propto 1/\theta$ FOR $\theta \ll 1$ AND $P_{\text{screen}}(\rho) \propto 1/\rho^2$, WHERE $P_{\text{screen}}(\rho)$ IS THE PROBABILITY OF A PIECE OF SCREEN TO HAVE THE OPTICAL DEPTH OF ρ. HOWEVER, WE ARE INTERESTED IN THE PROBABILITY DENSITY
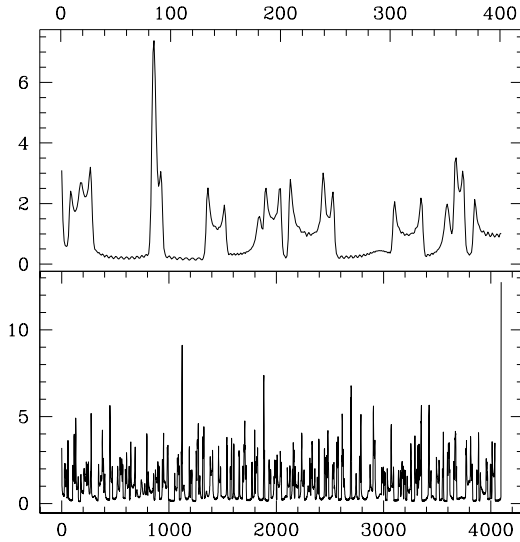
Figure 2. projected density. The upper panel is a zoom of the central portion of the lower panel. Each time the sheet folds in projection, we see a caustic structure in density.

Figure 3. deflection angle mapping. The horizontal axis is angle on the sky, and the vertical axis is the intersection of this light ray on the source plane. Whenever multiple different directions on the sky intersect on the same position in the source plane, multiple images are formed, which form a coherent interference pattern.

WITH RESPECT TO THE IMPACT PARAMETER, AND NOT WITH RESPECT TO THE LOCATION ON THE SCREEN. FOR NEARLY ALIGNED SCREENS, THIS IS NOT THE SAME THING. IN PARTICULAR, PART OF THE SCREEN WITH LOW θ OCCUPIES LESS OF THE IMPACT-PARAMETER SPACE THAN THE PART OF THE SCREEN WITH HIGH θ. THUS,

$$P_{\mathrm{impactparameter}}(\rho) \propto 1/\rho^3 \qquad (2)$$

STILL VERY NON-GAUSSIAN, BUT WITH THE SOFTER POWER-LAW. probability of a piece of screen is a highly non-Gaussian distribution, and resembles a Lorenzian, with divergent moments SO NOT THE LORENTZIAN, BUT SOFTER. The very high tails are cut off by higher order derivatives of the correlation function.

!!These high density caustics!! **The regions near the locations where the screen is parallel to the line-of-sight, which the call the caustics,** give rise to !!refractive lensing processes which resemble!! **the localized clumps in the pulsar's scattering image, which produce** the inverted parabolic arcs in pulsar secondary spectra.

4 LENSING

The lensing of this density sheet can be computed in analogy to Pen & King (2012).

Given the projected **column** density distribution in Figure 2, **and assuming that the sheet has a fixed optical depth along its normal**, we can compute the mapping of apparent angle on the sky to position in the source (pulsar) plane. The caustics in the projected density distribution lead to large angle deflections, and multiple imagine, whenever the sheets are aligned closer than the amplitude of the perturbations. This explains why only a small fraction of (edge-on) current sheets contribute to scintillation.
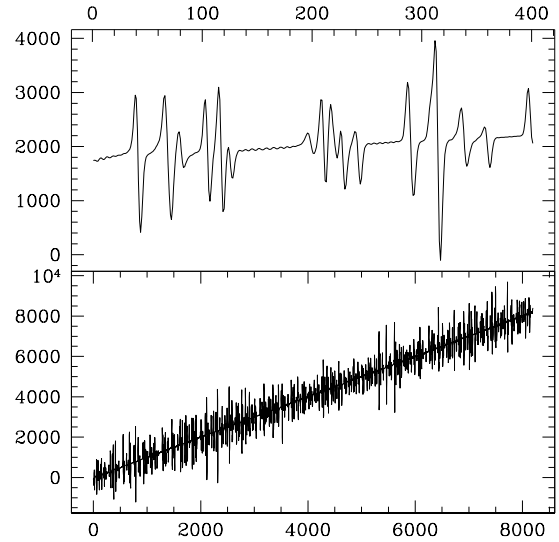
5 SIMULATED DYNAMIC SPECTRA

With the density field, we can solve the lens equations to simulate dynamic spectra. By adding the voltages on each image with their appropriate amplitude and phases, we simulate the dynamic spectrum, shown in figure 4. DO YOU WANT TO SAY A FEW WORDS ABOUT THE PROCEDURE THAT YOU USED TO GENERATE THE DYNAMICAL SPECTRA? IF YOU FOLLOWED SOMEBODY'S METHOD, DO YOU WANT TO REFER TO THIS PAPER?

A 2-D fourier transform maps this dynamic spectrum into a secondary spectrum, shown in figure 5.

We find that the interference of these discrete, co-linear images forms the inverted parabolic arcs, **qualitatively similar to those** that are observed **in Stinebring et al. (2001) and Hill et al. (2005), (2007).

6 DISCUSSION

We can estimate the length scales involved **in making the current sheet that would produce the observed scintillation pattern**. This theory requires as input a current sheet thickness, inclination angle, curvature, amplitude of waves, and dissipation scale.

The thickness of the sheets is determined by the magnification of images: the flux is roughly the thickness divided by the impact parameter WHY? NOT OBVIOUS TO READERS LIKE ME. It suggests a typical tickness of $h \sim 0.1$ AU WE SHOULD QUOTE SOME OBSERVATIONAL PAPER WHERE THESE MAGNIFICTIONS ARE MEASURED. A wave of projected wavelength $\alpha\lambda$ enhances projected densities by a factor $w = \sqrt{h\alpha\lambda}$ THIS FACTOR SHOULD BE DIMENSIONLESS. I GET $\sqrt{\alpha\lambda/h}$
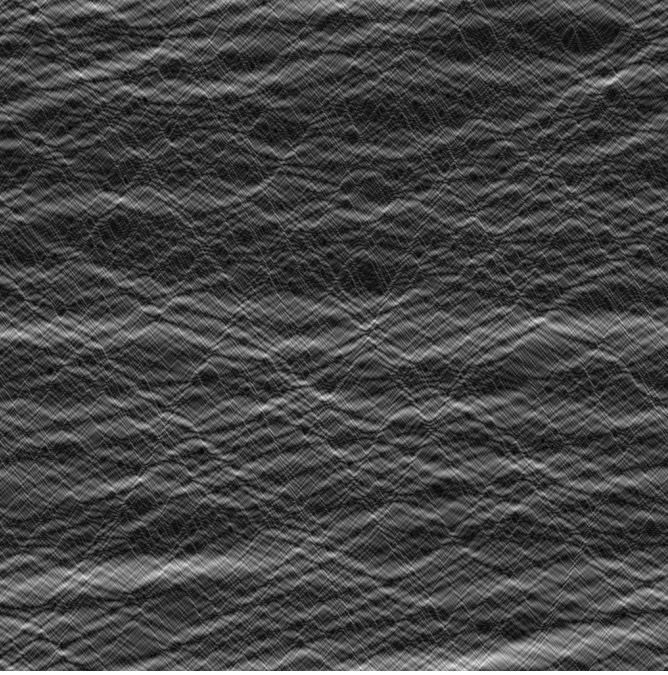
Figure 4. dynamic pulsar spectrum. Horizontal axis is time, vertical axis is frequency. We reproduce the characteristic criss-cross pattern observed in real scintillation spectra.
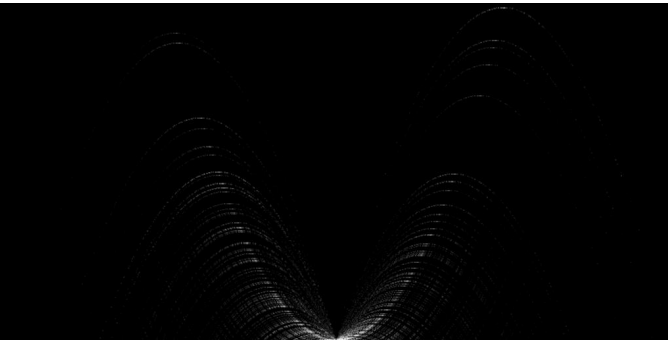

Figure 5. secondary pulsar spectrum. The inverted parabolic arcs arise naturally in this model.

The projected wavelengths are known to be of order ~ 10 AU, so $w \sim 10$. The largest deflection angles are $\gamma \sim 0.1$ mas, which requires a projected electron density change $\delta n_e/(w\alpha) \sim$??. In an underdense sheet, the maximal change of density is the density itself. For the mean interstellar medium densities determined from pulsar dispersion, we obtain $\alpha \sim 10^{-2}$. The probability of seeing a sheet at such an angle is $\sim \alpha^2$ I THINK IT SCALES $\propto \alpha$, NO? YOU ESSENTIALLY WANT THE NORMAL VECTOR TO THE SHEET BE WITIN α FROM 90 DEGREES, SO IF YOU ASSUME NORMAL VECTORS ARE ISOTROPICALLY DISTRIBUTED, YOU GET THE LINEAR SCALING WITH α, requiring the existence of $\sim 1/\alpha^2$ sheets along the line of sight SO I GET 100, NOT 10000. For B0834+06, the distance is ~ 1 kpc, giving a typical sheet separation of $s \sim 0.1$ pc. If we assume the curvature to be separation (it could be smaller), we find a limiting projection angle $\alpha_{\min} = \sqrt{h/s} \sim 0.002$. The wave amplitudes must be

$> \alpha\lambda$ in order to form projected caustics. This is a small amplitude, which rules out large amplitude universal turbulence. The latter would deform the sheet too much. In a Kolmogorov spectrum, the energy power spectrum scales as $k^{-5/3}$. Scaling from the alven damping scale to the fresnel scale, this results in density fluctuations $< 10^{-4}$. This is insufficient to create scintillation in pulsar fluxes.

These estimates are qualitative. One expects current sheets to come in a range of sizes, curvature and perturbation amplitude. The thickness might also vary, unless due to global resistivity.

UE-LI, I THINK ONE OF THE ATTRACTIVE FEATURES OF OUR MECHANISM IS THAT IT EXPLAINS VERY NATURALLY THE 1-D IMAGE OF BRISKEN ET AL. IMHO IT WOULD BE VERY GOOD IF YOU SHOWED THE 2-D SCATTERING IMAGE AND DEMOSTRATED THAT THE SCATTERING CLUMPS ARRANGE ALONG A LINE. IT MATTERS NOT THAT THIS RESULT IS PRELIMINARY AND WILL BE INVESTIGATED FURTHER; AS A PICTURE-SETTER, IT IS VERY IMPORTANT.

7 CONCLUSIONS

We have presented a quantitative theory of pulsar scintillation inverse parabolic arcs. These extend recent ideas of **Goldreich & Sridhar (2006) and Pen & King (2011) about** thin current sheets as the scattering objects in the ISM**, which naturally explain the large angle scattering observed in pulsars and some extragalactic sources.

This picture could explain all scintillation phenomena with structures greater than 0.1 AU. The apparent diffractive structure results from the interference between refractive images, and no diffractive scattering is needed.

8 ACKNOWLEDGEMENTS

REFERENCES

Braithwaite J., Spruit H. C., 2004, Nat, 431, 819
Brisken W. F., Macquart J.-P., Gao J. J., Rickett B. J., Coles W. A., Deller A. T., Tingay S. J., West C. J., 2010, ApJ, 708, 232
Cordes J. M., Rickett B. J., Stinebring D. R., Coles W. A., 2006, ApJ, 637, 346
Goldreich P., Sridhar S., 2006, ApJ, 640, L159
Hill A. S., Stinebring D. R., Asplund C. T., Berwick D. E., Everett W. B., Hinkel N. R., 2005, ApJ, 619, L171
Jain R., Roberts B., 1991, Solar Physics, 133, 263
Joarder P. S., Ghosh S. K., Poria S., 2009, Geophysical and Astrophysical Fluid Dynamics, 103, 89
Pen U.-L., King L., 2012, MNRAS, 421, L132
Scheuer P. A. G., 1968, Nat, 218, 920
Stinebring D. R., McLaughlin M. A., Cordes J. M., Becker K. M., Goodman J. E. E., Kramer M. A., Sheckard J. L., Smith C. T., 2001, ApJ, 549, L97

Walker M. A., 2007, in Haverkorn M., Goss W. M., eds, SINS - Small Ionized and Neutral Structures in the Diffuse Interstellar Medium Vol. 365 of Astronomical Society of the Pacific Conference Series, Extreme Scattering Events: Insights into the Interstellar Medium on AU-Scales. p. 299

Walker M. A., Koopmans L. V. E., Stinebring D. R., van Straten W., 2008, MNRAS, 388, 1214

Walker M. A., Melrose D. B., Stinebring D. R., Zhang C. M., 2004, MNRAS, 354, 43